

See discussions, stats, and author profiles for this publication at: <https://www.researchgate.net/publication/231657436>

Stochastic Effects on the Time-Dependent Rate Constant of Photodimerization of 12-(9-Anthroyloxy)stearic Acid in Micelles

ARTICLE *in* THE JOURNAL OF PHYSICAL CHEMISTRY · NOVEMBER 1996

DOI: 10.1021/jp9614660

CITATIONS

10

READS

9

3 AUTHORS, INCLUDING:



Maria João Moreno

University of Coimbra

47 PUBLICATIONS 545 CITATIONS

SEE PROFILE



Eurico Melo

New University of Lisbon

57 PUBLICATIONS 1,084 CITATIONS

SEE PROFILE

Stochastic Effects on the Time-Dependent Rate Constant of Photodimerization of 12-(9-Anthroyloxy)stearic Acid in Micelles

Maria João Moreno,[†] Isabel M. G. Lourtie,[‡] and Eurico Melo^{*,†}

Instituto de Tecnologia Química e Biológica and IST, Apartado 127, P-2780 Oeiras, Portugal, and Centro de Análise e Processamento de Sinais, IST, Av. Rovisco Pais, P-1096 Codex Lisboa, Portugal

Received: May 21, 1996; In Final Form: August 2, 1996[®]

We present a detailed study of the kinetics of photodimerization of 12-(9-anthroyloxy)stearic acid, 12-AS, in cetyltrimethylammonium chloride and polyoxyethylene(10) lauryl ether micelles. The primary objective of this study is to analyze the consequences of the distribution of reactant by the micelles on the reaction kinetics. It was found that the influence of stochastic effects on the photodimerization cannot, by itself, account for the deviation from a homogeneous media kinetics, and interchange of 12-AS molecules between micelles has to be invoked to explain the experimental data. Further, besides the stable head-to-tail dimer a non-negligible amount of a thermally unstable head-to-head photodimer is observed. It is concluded that the inhibition of photochemical bimolecular reactions, such as photodimerization, in compartmentalized media results from two factors: shortness of reactants within the mean displacement distance of the excited species and, in a more pronounced manner, the depletion of available reactants as reaction proceeds in the non-homogeneous media.

Introduction

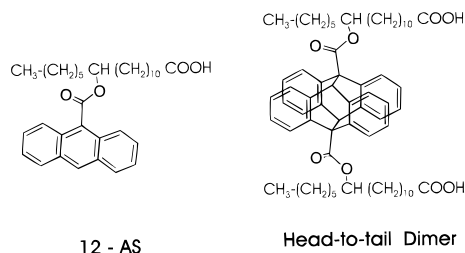
When reactants are confined in microcompartments in a non-homogeneous medium, the kinetics and chemical yield of bimolecular reactions differ considerably from those in continuous homogeneous media.¹ The restricted and closed reaction space produce two distinct effects: (i) the boundaries of the reaction compartment affect the diffusion of the reactants,^{2,3} and (ii) the limited number of available reactant molecules reduce the yield and modify the kinetics of the reaction.^{4,5} While being still a subject of research, the effect of geometrical confinement of the reaction volume, and consequent reduction of dimensionality, will not be focused on in this work. In this paper we are concerned with the stochastic effects upon the kinetics of bimolecular reactions taking place between substances incorporated in micelles, when the number of molecules per micelle is small.

The photocyclodimerization of anthracene and R-9-anthrates (R = Me, Et, Bz) is a well characterized singlet state photochemical reaction.^{6,7} For anthracene derivatives substituted in the 9 (meso) position this photochemical reaction yields two dimers, one head-to-tail (D_{ht}) and another head-to-head (D_{hh}). Only one final product, D_{ht}, has been observed when the reactant is a 9-anthroate ester.⁸ The photodimerization is nearly diffusion controlled in benzene. The dimer D_{ht} is thermally stable, and due to the saturation of the 9 and 10 carbons of the anthracene ring, it only absorbs in the benzenoid region.⁹ Upon absorption the dimer photodissociates to restore the two original monomer molecules.¹⁰ Therefore when the 9-anthroate moiety is excited with a longer wavelength, e.g. the 366 mercury line, no back reaction is observed.¹¹

The anthracene derivative 12-(9-anthroyloxy)stearic acid, 12-AS, incorporates into cationic or nonionic micelles, and in these micelles its chromophore resides in the hydrophobic core, to which the external water has a limited access.¹² The low content

of water of the environment results in a relatively long lifetime, increasing the reaction probability.

While anthracene and the previously mentioned R-9-anthrates, even at relatively low concentrations, produce a noticeable change in the light scattering of cetyltrimethylammonium bromide, CTAB, micelle solutions either before or after photodimer formation,¹³ we found that the fatty acid derivative 12-AS does not have the same effect, at least for the case of cetyltrimethylammonium chloride, CTAC, and polyoxyethylene(10) lauryl ether, C₁₂E₁₀, micelle solutions. Therefore we consider that the micelle properties are, in principle, not affected.



In CTAC cationic micelles and for pH > 5 the negatively charged acyl group of 12-AS is expected to lead to a negligible interchange of ground state reactants between micelles, a hypothesis that will be further criticized in this work. Due to its short lifetime, the interchange of excited 12-AS never has to be considered. For comparison, all experiments were also done in polyoxyethylene(10) lauryl ether, C₁₂E₁₀, nonionic micelles.

Kinetics of Photodimerization

Whenever a bimolecular step is involved in a reaction mechanism, for example in the case of a photodimerization, the distribution of the reactants in a non-homogeneous medium such as a micellar solution plays, for small occupancy numbers, a very important role. In fact, if there is no interchange of reactant between micelles, no reaction will occur in those micelles occupied by a single reactant molecule. For occupation numbers greater than 1, the reaction will proceed with a speed

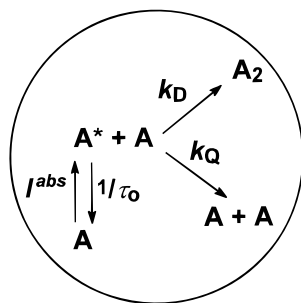
* To whom correspondence should be addressed.

[†] Instituto de Tecnologia Química e Biológica and IST.

[‡] Centro de Análise e Processamento de Sinais, IST.

[®] Abstract published in *Advance ACS Abstracts*, November 1, 1996.

SCHEME 1



SCHEME 2

Molecular Reaction		Micelle Notation
$A \rightarrow A^*$	I^{abs}	$M_{i+1} \rightarrow M_i^*$ $I^{abs}(i+1)[M_{i+1}]/[A]$
$A^* \rightarrow A$	$1/\tau_0[A^*]$	$M_i^* \rightarrow M_{i+1}$ $1/\tau_0[M_i^*]$
$A^* + A \rightarrow A + A$	$k_Q[A^*][A]$	$M_i^* \rightarrow M_{i+1}$ ${}^1k_Q i[M_i^*]$
$A^* + A \rightarrow A_2$	$k_D[A^*][A]$	$M_i^* \rightarrow M_{i-1}$ ${}^1k_D i[M_i^*]$

that, in the absence of other effects, is proportional to the number of reactant molecules. Moreover, in all the micelles with an odd occupation number a single molecule remains without possibility of reaction after reaction completion.^{14,15}

By analogy with what has been observed in homogeneous media the photodimerization of 12-AS in the presence of micelles, by irradiation with the 366 nm mercury line of intensity I^0 , of which I^{abs} is absorbed, may be represented by the general kinetic Scheme 1.

While the unimolecular deexcitation pathways, represented together in the $1/\tau_0$ rate step, are not affected themselves by the compartmentalization, the bimolecular reactions leading to the dimer, k_D , and to deexcitation, k_Q , are highly hindered by the isolation of reagents into noncommunicating compartments.

The photodimerization mechanism from Scheme 1 is alternatively represented by Scheme 2, where the micelle notation describes the consequence in the micelle population of a molecular reaction event. In this notation the reactant, A, is distributed by compartments M (e.g. micelles), and M_i denotes a reaction compartment with i molecules of reactant in the ground state, A, and M_i^* represents a reaction compartment with i molecules of reactant in the ground state, A, and one excited molecule, A^* (e.g. a 12-AS molecule in the singlet excited state).

The units of 1k_D and 1k_Q in Scheme 2 are s^{-1} , and these pseudounimolecular rate constants relate with the corresponding bimolecular rate constants, k_D and k_Q , through the volume of the reaction compartment. In the case of micelles of molar volume V_M , ${}^1k_D = k_D/V_M$ and ${}^1k_Q = k_Q/V_M$.^{14,16}

In our analysis the time evolution of the concentration of A is deduced under the following assumptions: (i) All micelles have identical volume and shape. (ii) There is no change in the characteristics of the micelles due to the presence of the solute. (iii) The effect of the geometrical confinement on diffusion (Smoluchovski-like transient effects) is not considered. That is, k_D and k_Q (as well as 1k_D and 1k_Q) are time independent.

Reactions of the Scheme 2 lead to the following set of differential equations:

$$\frac{d[M_i]}{dt} = -I^{abs} i[M_i]/[A] + \frac{1}{\tau_0}[M_{i-1}^*] + {}^1k_Q(i-1)[M_{i-1}^*] + {}^1k_D(i+1)[M_{i+1}^*] \quad (1)$$

$$\frac{d[M_i^*]}{dt} = I^{abs}(i+1)[M_{i+1}]/[A] - \left(\frac{1}{\tau_0} + i^1k_Q + i^1k_D\right)[M_i^*]$$

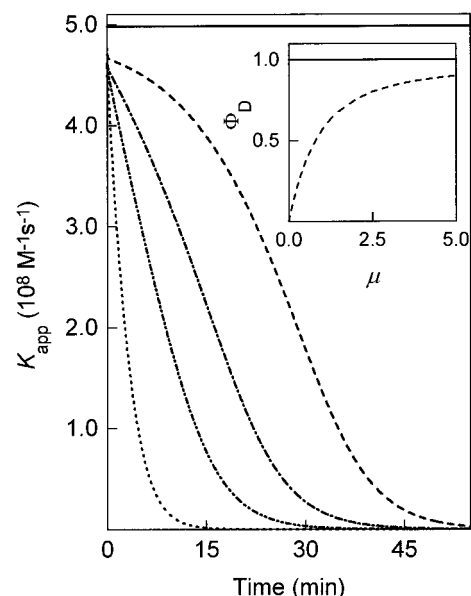


Figure 1. Theoretical simulation with the rate constants, $I^0 = 1.8 \times 10^{-4}$, $\tau_0 = 10$ ns, $k_{SQ} = 1 \times 10^9$, and $\gamma = 0.05$. Variation of the apparent dimerization rate constant, $k_{app} = (d[A_2]/dt)/[A][A^*]$, with reaction time, for a Poisson distribution of reactant into micelles and a mean occupation value of 0.3 (···), 1.0 (---), 2.0 (-·-), and 5.0 (---); and for a homogeneous phase with the same characteristics of the micelle media (—). Inset: efficiency of dimerization in the homogeneous (—), and compartmentalized (---) system, as a function of the mean occupation number.

to be solved with initial conditions

$$[M_i^*]_{t=0} = \frac{I^{abs}(i+1)[M_{i+1}]_{t=0}}{[A](1/\tau_0 + i^1k_Q + i^1k_D)} \quad \text{steady-state condition (2a)}$$

$$[M_i]_{t=0} = [M] \frac{\mu^i e^{-\mu}}{i!} \quad \text{Poisson distribution (2b)}$$

or

$$[M_i]_{t=0} = [M] \frac{n!}{i!(n-i)!} p^i q^{n-i} \quad \text{binomial distribution (2c)}$$

where $[M] = \sum_{i=0} [M_i]$, μ is the mean occupation number, $\mu = [A]/[M]$, $p = \mu/n$, $q = (1-p)$, and n is the maximum number of molecules per micelle.

In the system of differential equations (1) we do not need to consider occupation numbers i beyond values for which the concentration of reactant $i[M_i]$ is below our experimental accuracy, say $i[M_i]/[M] \leq 10^{-3}$. Therefore, eqs 1 do represent, in practice, a finite set of differential equations that can be solved numerically in the usual way. For the numerical integration it is wise to use a method that can deal with stiff systems, which is likely to be the case for most practical sets of rate constants.¹⁷

It is important to clarify that, since we know τ_0 and $k_{SQ} = (k_D + k_Q)$ from fluorescence decay analysis, the only fitting parameter is k_D .

Figure 1 illustrates the difference in the kinetics of the disappearance of monomer and formation of dimer theoretically calculated according to the described model for a set of rate constants characteristic of the system we are studying. As expected, in micelles the concentration of dimer tends asymptotically to a much lower value than in a comparable homogeneous media, and an equivalent limiting concentration of unreacted monomer is thus obtained. The apparent rate constant of dimerization defined as $k_{app}(t) = (d[A_2]/dt)/[A][A^*]$ allows a direct comparison of the kinetics of the reaction in homoge-

neous and compartmentalized media. There is a striking difference between the constancy of k_{app} in homogeneous media and its fast decrease in heterogeneous media. In the Results and Discussion section we test the concordance between the predictions of this model and our experimental findings.

Materials and Methods

For all solutions 10^{-2} M sodium phosphate buffers in Millipore water were used. Solutions of CTAC were buffered at pH = 6, and solutions of C₁₂E₁₀ were at pH = 7.2. These last also contained NaCl (10^{-1} M). All solvents are spectroscopic or HPLC grade from Merck or Riedel-de Haën. 12-AS is from Molecular Probes, and the surfactant C₁₂E₁₀ is from Sigma Chemicals; both were used without further purification. The surfactant CTAC, a gift from Irmãos Planas Almasqué, Lda., Lisboa, was extracted from Arquard 16-29 from Akzo Chemicals, Amersfoort, and was lyophilized before use. All measurements have been performed either at 20 ± 1 or at 30 ± 1 °C. The value of critical micelle concentration, cmc, for CTAC in our experimental conditions, $(1.4 \pm 0.1) \times 10^{-3}$ M, was obtained from literature.¹⁸ The aggregation number, ν , for these micelles was obtained by interpolation of literature values;¹⁸ ν (CTAC) = 117 for a surfactant concentration of 0.12 M. The molar micelle volume, V_M , for the same surfactant was also obtained by interpolation of the hydrodynamic radii given by Offen et al.;¹⁹ for the conditions given above V_M (CTAC) = 80 M⁻¹. The CTAC micelles are known to have a low dispersivity and spherical shape at least for [CTAC] < 1.2 M.¹⁸ The values for C₁₂E₁₀ were taken from literature;²⁰ cmc = 10^{-4} M, ν (C₁₂E₁₀) = 62, and V_M (C₁₂E₁₀) = 100 M⁻¹.

The kinetics of photodimerization was carried out with a 50 W Hg lamp in a PTI focusing lamp housing. For irradiation of CTAC solutions, the irradiation wavelength range was set by interposing in the light beam a thin glass plate transmitting $\lambda > 330$ nm; the intensity was controlled using neutral density filters. The absorbed light was, therefore, essentially constituted by the 366 nm mercury line and a small amount of 404 nm, the higher λ 's not being absorbed by 12-AS. The total light absorbed was determined by calculating the overlap between the absorption and lamp plus filter light spectrum, whose intensity was determined by potassium ferrioxalate actinometry. The intensity obtained without neutral density filter was $I^0 = 1.0 \times 10^{-6}$ einstein s⁻¹, and with a filter of 0.5 OD, $I^0 = 3.5 \times 10^{-7}$ einstein s⁻¹. For irradiation of C₁₂E₁₀ solutions a 366 nm filter was used in addition to the setup described above, and the intensity obtained was $I^0 = 2.5 \times 10^{-7}$ einstein s⁻¹.

In the photodimerization experiment, a micelle solution of volume of 5.5 cm³, equilibrated with air, was forced to circulate between the irradiation cell (optical path $l = 1$ cm, $V = 2.5$ cm³) and an analysis cell ($l = 0.15$ cm) placed in a spectrophotometer, where the disappearance of 12-AS was followed at 364 nm. The circulation was done using a peristaltic pump (Pharmacia LKB, Pump P-1), at a rate of approximately 10 mL min⁻¹.

Analysis of irradiation products was performed by HPLC with a diode array absorption detector (Merck-Hitachi) and by TLC.

Absorption spectra were obtained with a Beckman DU-70. The time evolution of 12-AS and dimer concentrations were calculated by numerical integration of eq 1 or 6 using the Gear method for numerical solution of stiff differential equations.¹⁷ The fit of eq 1 or 6 to the experimental data was done with the help of the Simplex algorithm.²¹ All calculations were performed on a personal computer using FORTRAN routines.

Steady state fluorescence spectra were obtained using a SPEX Fluorolog 212, and time-resolved fluorescence experiments were

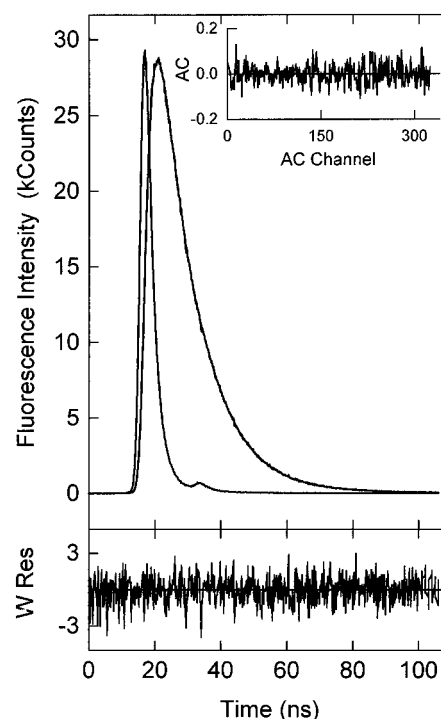


Figure 2. Lifetime decay of 12-AS in CTAC, $\mu = 1.0$, and best fit with the exp-of-exp law, eq 3. The recovered fit parameters are present in Table 1.

obtained by time-correlated single-photon counting with an experimental setup described elsewhere.²²

Solubility values were obtained using both UV absorption spectroscopy and HPLC of saturated solutions equilibrated for at least 48 h at the required temperature and separated by filtration through a 0.45 μ m pore diameter PTFE membrane.

Results and Discussion

The fluorescence decay of 12-AS in micellar solutions of CTAC or C₁₂E₁₀ for $\mu = 0.03$ follow the usual pattern.¹² Due to the rotation of the anthracene group with respect to the carboxylate group, the time-resolved fluorescence presents a rise time $\tau_1 \leq 1$ ns for wavelengths longer than 470 nm in CTAC and 465 nm in C₁₂E₁₀ and a concomitant fast decay for shorter wavelengths. In CTAC, at 470 nm the components arising from the appearance of the planar form stable in the excited state and from disappearance of the twisted species cancel, and a single-exponential decay with a lifetime identical to that of the relaxed form is obtained.¹² In C₁₂E₁₀ the same behavior is observed at 465 nm. All subsequent work has been done at these "magic" wavelengths.

When the number of 12-AS molecules per micelle is higher, the decays cannot be fitted to a single-exponential law but may be successfully adjusted to a exp-of-exp law (3)²³ which is valid for a Poisson distribution of molecules by the micelles, Figure 2 and Table 1.

$$I_F(t) = I_F(0) \exp \left\{ -\frac{t}{\tau_0} - \mu [1 - \exp(-k_{SQ}t)] \right\} \quad (3)$$

In C₁₂E₁₀ there is an excellent fit to eq 3 for concentrations up to $\mu = 2$ without any significant variation of the unquenched lifetime. In the case of CTAC there is a noticeable change in τ_0 , for $\mu \geq 1.0$, which may be symptomatic of the occurrence of perturbation of the micelles.

The value of the self-quenching rate constant obtained does not change significantly with reactant concentration, which is

TABLE 1: Unquenched Lifetime, τ_0 , and Self-Quenching Rate Constant, k_{SQ} , of 12-AS in Micelles of CTAC and C₁₂E₁₀^a

surfactant	μ	T (°C)	Poisson distribution		binomial distribution $n = 3$	
			τ_0 (ns)	k_{SQ} (10 ⁹ M ⁻¹ s ⁻¹)	τ_0 (ns)	k_{SQ} (10 ⁹ M ⁻¹ s ⁻¹)
CTAC	0.03	20	10.4 ± 0.1		10.4 ± 0.1	
	0.3		10.7 ± 0.1	0.9 ± 0.2	10.7 ± 0.1	1.2 ± 0.2
	1.0		11.3 ± 0.1	0.8 ± 0.1	11.2 ± 0.1	1.2 ± 0.1
	1.6		11.7 ± 0.1	0.7 ± 0.1	11.9 ± 0.1	1.2 ± 0.1
	2.0		11.9 ± 0.1	0.9 ± 0.1	12.4 ± 0.1	1.6 ± 0.1
C ₁₂ E ₁₀	0.03	30	11.2 ± 0.1		11.2 ± 0.1	
	0.5		11.4 ± 0.1	0.9 ± 0.2	11.3 ± 0.1	1.3 ± 0.2
	1.0		11.6 ± 0.1	0.9 ± 0.1	11.6 ± 0.1	1.4 ± 0.1
	2.0		11.9 ± 0.1	0.9 ± 0.1	12.4 ± 0.1	1.6 ± 0.1

^a In all calculations the value of the unquenched lifetime, τ_0 , was left free to adjust. The results are obtained with the equation law for a Poisson distribution and a binomial distribution of 12-AS by the micelles, eqs 3 and 4, respectively.

an indication that the model used for the analysis of the decays is adequate. However, the fact that the limiting solubility of 12-AS in CTAC does not attain $\mu = 2$ and the dependence of τ_0 with μ lead us to test the hypothesis that the use of a binomial distribution, instead of a Poisson distribution, could give a better description of our decays. The results obtained with the binomial law, eq 4, are also presented in Table 1. For CTAC there is, as expected, an increase of the k_{SQ} values relative to the ones obtained with eq 3, but the values of τ_0 for $\mu \geq 1.0$ are still anomalous. Only on the basis of this data, we cannot judge which model better describes the decay in CTAC micelles. For C₁₂E₁₀ the incoherence of τ_0 required for the minimization of the fit parameter χ^2 indicates that in these micelles the binomial model is inappropriate for the analysis of the experimental data.

$$I_F(t) = I_F(0) \sum_{i=1}^n \left\{ \frac{i}{\mu} \frac{n!}{i!(n-i)!} p^i q^{n-i} \exp \left[-\frac{t}{\tau_0} - (i-1)k_{SQ}t \right] \right\} \quad (4)$$

Experimental and predicted steady state fluorescence emission intensities are in good agreement within experimental accuracy. Therefore there is no evidence for any ground state association such as static quenching (results not shown). The agreement between steady state and time-resolved data also shows that the transient effects need not be taken into account.

Preparative irradiation of 12-AS in a homogeneous medium, 1,4-dioxane, gave a single HPLC final product identified as the head-to-tail dimer. The possibility of formation of other products of the irradiation of 12-AS in CTAC and C₁₂E₁₀ micelles, namely, reaction with the surfactant and photoreaction with O₂, was equally inspected by quantitative HPLC analysis. In all the experiments the disappearance of monomer could be quantitatively ascribed to a concomitant dimer formation.

The kinetics of dimerization of 12-AS in micelles was followed by continuous monitoring of solution absorption at the 364 nm absorption band as described in the Materials and Methods section.

To ascertain that the rate constants obtained from the photodimerization characterize the reaction kinetics adequately, we used three different concentrations of 12-AS: $\mu_{t=0} = 0.30$, 1.0, and 1.6 in CTAC and $\mu_{t=0} = 0.50$, 1.0, and 2.0 in C₁₂E₁₀. With identical purpose two different irradiation light intensities, $I^0 = 1.8 \times 10^{-4}$ and 6.4×10^{-5} einstein s⁻¹ dm⁻³, have been used in the experiments with CTAC.

TABLE 2: Rate Constants for $t = 0$, $k_D(t=0)$, for Steady State Photodimerization, Using τ_0 and k_{SQ} Obtained from Fluorescence Time-Resolved Measurements^a

surfactant	μ	$k_D(t=0)$ (10 ⁷ M ⁻¹ s ⁻¹)		
		homogeneous	Poisson distribution	binomial distribution $n = 3$
CTAC	0.3	2.2	2.4	3.7
	0.94	2.1	2.3	3.5
	1.6	2.0	2.2	3.2
	2.0	1.8	2.1	3.1
C ₁₂ E ₁₀	0.5	8.2	9.0	
	1.0	8.1	8.8	
	2.0	7.8	8.4	

^a $T = 30$ °C and $I^0 = 4.5 \times 10^{-5}$ einstein⁻¹ s⁻¹ dm⁻³ for the C₁₂E₁₀ micelle solution. $T = 20$ °C, $I^0 = 6.4 \times 10^{-5}$ and 1.8×10^{-4} einstein⁻¹ s⁻¹ dm⁻³ for the CTAC micelle solution; the same rate constants have been obtained for both intensities of light irradiation.

The analysis of the initial rate of disappearance of monomer gives approximated k_D values. The obtained value depends on the model used for the analysis. See, eqs 5:

$$\left(\frac{d[A_2]}{dt} \right)_{t=0} = {}^1k_D \mu \frac{I^{abs}}{1/\tau_0 + {}^1k_{SQ}\mu} \quad \text{homogeneous media} \quad (5a)$$

$$\left(\frac{d[A_2]}{dt} \right)_{t=0} \cong \sum_{i=1}^{i_{max}-1} {}^1k_D i [M_i^*] \quad \text{Poisson distribution} \quad (5b)$$

where $[M_i^*]$ is obtained from eqs 2. For the case of a binomial distribution of reactant among the micelles, in eq 5b i_{max} is replaced by n .

The rate constants experimentally obtained for a Poisson distribution do not differ appreciably from those for a homogeneous media analysis; the same is not true in the case of a binomial distribution, which leads to higher values for the dimerization rate constant, Table 2.

Simulation of eqs 5a and 5b with several rate constants lead us to conclude that, if the mean displacement of the reactant during the excited state, $\sqrt{3D\tau_0}$, where D is the diffusion coefficient, is much smaller than the dimensions of the micelle, the initial rate of dimer formation is the same for a homogeneous media and for a Poisson distribution. However, if it is similar or higher than the dimensions of the reaction compartment, the initial rate of dimer formation is smaller in the case of a compartmentalized reaction space (for a given experimental rate of dimer formation the recovered rate constant will be higher). This may be rationalized in the following way: in homogeneous media, the initial random distribution of ground state molecules around an excited molecule follows a Poisson distribution, and if the product of the diffusion coefficient by the excited state lifetime is too small, the molecules have no time to feel the boundaries of the reaction compartment and the rate equations collapse in the homogeneous media ones, Figure 3.

A larger difference is observed if we model the distribution of reactants as binomial, Table 2. The interpretation is qualitatively identical to the one presented for the Poisson distribution.

When a fit of the overall disappearance of monomer to the kinetics presented in Scheme 2 and described by eqs 1 was attempted, the plot indicates a clear disagreement between models and experimental data, Figure 4. Furthermore, the recovered rate constants obtained from the best fits are concentration and light intensity dependent, and the extent of the reaction for long times is much higher than that predicted, providing evidence for the incompleteness of the reaction

SCHEME 4

Molecular Reaction		Micelle Notation	
$A \rightarrow A^*$	I^{abs}	$j,k M_{i+1} \rightarrow j,k M_i^*$	$I^{abs}(i+1)[j,k M_{i+1}]/[A]$
$A^* \rightarrow A$	$1/\tau_0[A^*]$	$j,k M_i^* \rightarrow j,k M_{i+1}$	$1/\tau_0[j,k M_i^*]$
$A \rightarrow A_w$	$k^-[A]$	$j,k M_i \rightarrow j,k M_{i-1}$	$k^-i[j,k M_i]$
$A_w \rightarrow A$	$k^+[A_w][M]$	$j,k M_i \rightarrow j,k M_{i+1}$	$k^+[A_w][j,k M_i]$
$A^* + A \rightarrow A + A$	$k_Q[A^*][A]$	$j,k M_i^* \rightarrow j,k M_{i+1}$	${}^1k_Q i[j,k M_i^*]$
$A^* + A \rightarrow D_{ht}$	$(1 - f_{Dhh})k_D[A^*][A]$	$j,k M_i^* \rightarrow (j+1),k M_{i-1}$	$(1 - f_{Dhh}){}^1k_D i[j,k M_i^*]$
$A^* + A \rightarrow D_{hh}$	$f_{Dhh}k_D[A^*][A]$	$j,k M_i^* \rightarrow j,(k+1)M_{i-1}$	$f_{Dhh}{}^1k_D i[j,k M_i^*]$
$D_{hh} \rightarrow A + A$	$k_R[D_{hh}]$	$j,k M_i \rightarrow j,(k-1)M_{i+2}$	$k_R k[j,k M_i]$

molecules of reactant A in the ground state, j molecules of dimer D_{ht} , and k molecules of dimer D_{hh} ; $j,k M_i^*$ is a reaction compartment with i molecules of reactant A, j molecules of D_{ht} , k molecules of D_{hh} , and one molecule of A^* (e.g. a 12-AS molecule in the singlet excited state).

Equations of Scheme 4 lead to the following set of differential equations:

$$\frac{d[j,k M_i]}{dt} = -I^{abs}i[j,k M_i]/[A] + \frac{1}{\tau_0}[j,k M_{i-1}^*] + {}^1k_Q(i-1)[j,k M_{i-1}^*] + (1 - f_{Dhh}){}^1k_D(i+1)[j-1,k M_{i+1}^*] + f_{Dhh}{}^1k_D(i+1)[j,k-1 M_{i+1}^*] + k_R(k+1)[j,k+1 M_{i-2}] + [A_w]k^+([j,k M_{i-1}] - [j,k M_i]) + k^-[(i-1)[j,k M_{i-1}] - i[j,k M_i]] \quad (6)$$

$$\frac{d[j,k M_i^*]}{dt} = I^{abs}(i+1)[j,k M_{i+1}]/[A] - \left(\frac{1}{\tau_0} + i{}^1k_Q + i{}^1k_D\right)[j,k M_i^*]$$

This set of equations can be solved for the same initial conditions used for eq 1, and despite its apparent complexity since only the first few occupation numbers have to be considered and only two parameters are adjustable, the numerical integration of the finite set of equations so obtained is feasible.

We consider that every encounter of 12-AS negative molecule with a micelle leads to association between them, and for a micelle with a hydrodynamic radius R_M and a 12-AS molecule with radius R_{12-AS} , $k^+ = 2N_A(R_M + R_{12-AS})^2 kT/3000\eta R_M R_{12-AS}$. In this way, the calculated values of k^+ are 1.2×10^{10} and 1.6×10^{10} respectively for CTAC and $C_{12}E_{10}$. In the case of a binomial distribution the entrance rate, k_{bin}^+ , is dependent on the number of reactant molecules already present in the micelle and, assuming that for the first molecule the entrance rate is diffusion controlled, is given by²⁵ $k_{bin}^+ = (n - i - 2(j + k))(k^+/n)$.

The new processes introduced by Scheme 3 do not modify the fluorescence decay analysis whose results are depicted in Table 1 because the dynamics of 12-AS entrance and exit of micelles is a slow process in the time scale of the lifetime measurements.²⁶ Therefore each micelle can be considered a microcompartment where reactants are isolated, and the system is adequately described by Scheme 2. The same is true for the steady state photodimerization for $t = 0$.

In Figure 6a the decrease of concentration of 12-AS with the time of irradiation with light 6.4×10^{-5} einstein $s^{-1} dm^{-3}$ of a solution 10^{-3} M in CTAC micelles, and $\mu_{t=0} = 0.30$, is depicted together with the weighted residuals (${}^1k_D = 2.2 \times 10^5 s^{-1}$ and $k^- = 0.9 \times 10^{-3} s^{-1}$). A similar fit is presented in Figure 6b but for a solution with the same surfactant concentration and $\mu_{t=0} = 1.0$ (${}^1k_D = 2.2 \times 10^5 s^{-1}$ and $k^- = 0.5 \times 10^{-3} s^{-1}$). The rate constants obtained for different light intensities and different mean occupation numbers are presented in Table 3.

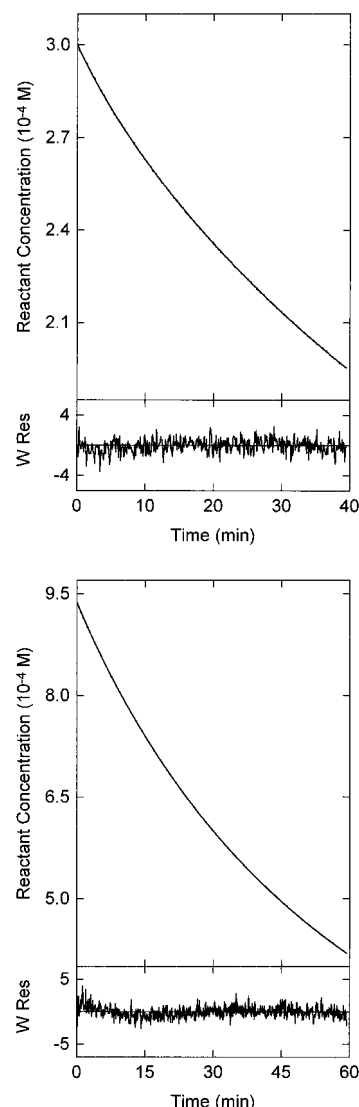


Figure 6. Fit of the variation of 12-AS concentration with time (···) by irradiation with $I^0 = 6.4 \times 10^{-5}$ einstein $s^{-1} dm^{-3}$ of solutions (a, top) with $\mu_{t=0} = 0.3$ and (b, bottom) $\mu_{t=0} = 1.0$, to the theoretically predicted variation (—), eqs 6 and 2. The weighted residues are also presented.

TABLE 3: Steady State Photodimerization Rate Constant, k_D , and Exit Rate Constant, k^- , Obtained from the Best Fit of Eqs 6 and 2 to Experimental Results, Using τ_0 and k_{SQ} Obtained from Fluorescence Time-Resolved Measurements

surfactant	I^{abs} (eins $s^{-1} dm^{-3}$)	μ	Poisson distribution		binomial $n = 3$	
			k_D ($10^7 M^{-1} s^{-1}$)	k^- ($10^{-3} s^{-1}$)	k_D ($10^7 M^{-1} s^{-1}$)	k^- ($10^{-3} s^{-1}$)
CTAC	1.8×10^{-4}	0.30	2.2	1.2	4.8	1.5
		0.94	2.3	0.7	4.2	0.7
		1.60	2.2	0.6	3.9	~0.0
	6.4×10^{-5}	0.30	2.2	0.9	5.0	1.2
		0.94	2.2	0.5	3.9	0.5
$C_{12}E_{10}$	4.5×10^{-5}	1.60	2.2	0.3	3.9	~0.0
		0.5	9.4	3		
		1.0	8.9	4		
		2.0	8.4	3		

In Figure 7 the experimental variation of reactant concentration with the time of irradiation for $I^0 = 1.8 \times 10^{-4}$ einstein s^{-1} and different values of $\mu_{t=0}$ is compared. The superimposed curves are the theoretical predictions obtained from eqs 6 and 2 with the Poisson distribution statistics. The dimerization rate constant obtained is independent of the mean occupation number and of the irradiation light intensity. The variation of the exit

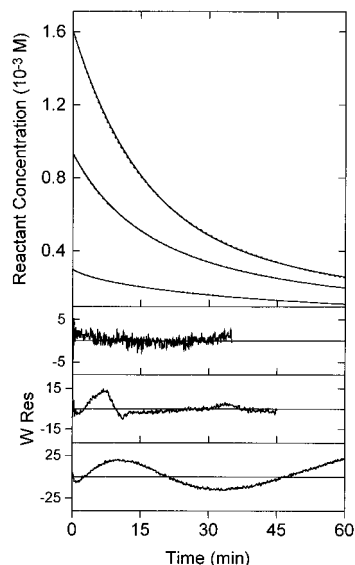


Figure 7. Comparison of the variation of reactant concentration with time, by irradiation with $I^0 = 1.8 \times 10^{-4}$ einstein $\text{s}^{-1} \text{dm}^{-3}$, for three different initial mean occupation numbers. The weighted residues of the best fit are also presented, from the bottom to top: $\mu_{t=0} = 1.6$, $\mu_{t=0} = 1.0$, and $\mu_{t=0} = 0.3$.

rate constant will be discussed later. In $\text{C}_{12}\text{E}_{10}$ the fit is good for all conditions, and the agreement between the recovered rate constants for all μ is an indication that the system is adequately described by the proposed model.

The fit of eqs 6 assuming a binomial distribution is not as good as the one obtained for a Poisson distribution, and the rate constants obtained are incoherent, which indicates that reactant distribution in both micelle systems is best described by a Poisson distribution.

The efficiency of photodimerization, defined as $\gamma = k_D/k_{SQ}$, is quite different for the two tested micelles: $\gamma \approx 0.03$ for CTAC, and $\gamma \approx 0.10$ for $\text{C}_{12}\text{E}_{10}$. According to the reaction Scheme 5, which includes the diffusion-controlled formation and dissociation of the encounter complex, the efficiency of photodimerization is $\gamma = k_D'/(k_D' + k_Q')$. Within the context of this model γ is only dependent on the relative probabilities of dimerization and quenching after the encounter species is generated. A similar value has been determined for the dimerization of benzyl 9-anthroate, $\gamma = 0.06$, in homogeneous media (benzene).⁶ The higher value obtained for 12-AS in $\text{C}_{12}\text{E}_{10}$ is not surprising since in benzyl 9-anthroate the benzyl group may hinder the dimerization step. In support of this interpretation is ethyl 9-anthroate in benzene, $\gamma = 0.2$.²⁷ The comparatively low value obtained in CTAC is probably the result of a hindered collision conformation due to the anchoring of the fatty acid head group at the surface of these micelles.

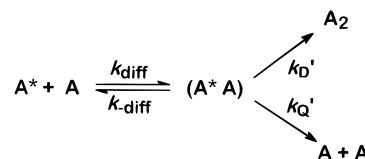
To obtain an estimate of the equivalent viscosity of the micelle reaction media, we can relate the dimerization rate constant, k_D , with the solvent viscosity by using the encounter complex model, Scheme 5. k_D is related to the individual rate constants by equation 7.²⁸

$$k_D = \frac{k_{\text{diff}} k_D'}{k_{\text{-diff}} + k_D' + k_Q'} \quad (7)$$

where $k_{\text{diff}} = 4\pi N_A R D / 1000$, $k_{\text{-diff}} = 3D/R^2$ in the case of a null binding energy for the encounter complex, and $D = 2 \times 10^6 \text{ kT} / 3\pi\eta R f_i$.

In homogeneous media (benzene) the dimerization rate constant for benzyl 9-anthroate is $k_D = 6 \times 10^8 \text{ M}^{-1} \text{s}^{-1}$. Using the above equations for the comparison between k_D in benzene

SCHEME 5



and the values found in this study (CTAC $k_D = 2 \times 10^7$, $\text{C}_{12}\text{E}_{10}$ $k_D = 9 \times 10^7$) and assuming that $k_D' + k_Q'$ does not change, we find a micelle viscosity of about 17 cP in both micelle systems. Having in mind the dubious significance of the viscosity inside the micelle and the applicability of homogeneous media equations to micelle solutions, the above value is reasonable.²⁹

In Scheme 5 we postulate that the encounter complex can dimerize without the intermediacy of any other species, namely, an excimer. While there is no experimental evidence that an excimer is formed as an intermediate in the photodimerization, it is important to demonstrate that, if it is formed, it will not interfere with the kinetic analysis presented here.

The presence of an emissive excimer is out of question since we did not find any change in the emission spectra for the highest concentrations used in micelles. Moreover, intramolecular bis(9-anthroates) connected by 1, 2, 3, 5, and 6 methyl groups exhibit the same emission spectra as the parent compound, ethyl 9-anthroate.³⁰

A reversible but nonemissive excimer should reveal itself in the fluorescence decay of the monomer as a positive or negative new component depending on the lifetime of the excimer. The fluorescence decays in micelles fit perfectly the exp-of-exp law without having to add any new component at high 12-AS concentrations. In addition, those bichromophoric 9-anthroates used by A. Maçanita besides the decrease of fluorescence lifetime due to intramolecular quenching do not show any new component in the fluorescence decay.³⁰ Therefore, if a non-emissive excimer is formed, its reversibility does not compete with the efficient self-quenching plus dimerization steps.

In any case, some strong interaction between two colliding molecules must exist in order to explain the high self-quenching efficiency observed. This "intermediate" may be excimeric or not. At 77 K sandwich dimers of benzyl 9-anthroate display excimer emission with a maximum at 500 nm, but the stabilization enthalpy of this excimer is only ca. -12 kJ/mol ,³¹ therefore not enough to compensate for the entropy destabilization at room temperature, which for similar excimers is ca. 20 kJ/mol .³² This result argues in favor of an excimer-like encounter complex.

The observed increase of the unquenched lifetime of 12-AS with μ is not negligible, in particular in CTAC micelles. The excited state of anthroate derivatives is known to be strongly quenched by water, and these probes have been used to determine the concentration of water inside micelles and phospholipid bilayers.^{12,22} In this way the lifetime variation may reflect a structural change of the micelle, with a decrease in the water penetration. The exit rate constant, k^- , shows also a small decrease with the increase of μ . This may also be a consequence of the modification of the structural characteristics of the micelle. The lower variation of unquenched lifetime and exit rate constant observed in $\text{C}_{12}\text{E}_{10}$ is evidence for a smaller perturbation of these micelles by the addition of 12-AS. Besides the interchange of reactants between micelles through the water, the randomization could also take place by coalescence of micelles, which could justify the decrease in the exit rate constant observed. However, this mechanism should be much more important for the $\text{C}_{12}\text{E}_{10}$ case, where k^- is constant for the entire concentration range.

Obviously the number of 12-AS molecules that do not strongly disturb a micelle is very small, and several studies have clearly demonstrated this.^{19,33} Moreover, we found that the limiting solubility of 12-AS in 0.12 M CTAC is less than 2×10^{-3} M ($\mu = 2$). In general, the solubility of a compound in a micelle solution is limited by both its solubility in the micelle pseudophase (maximum number of molecules per micelle) and in the aqueous phase. In the case of our more concentrated solutions in CTAC, for which $\mu = 1.6$ and $[M] = 10^{-3}$ M, the concentration of 12-AS in the aqueous pseudophase, $[12\text{-AS}_w]$, calculated using the entrance and exit rate constants from our model fits, is on the order of 10^{-13} M ($[12\text{-AS}_w](\text{Poisson}) = 1.6 \times 10^{-13}$ M, $[12\text{-AS}_w](\text{binomial } n = 3) = 3.4 \times 10^{-13}$ M, and $[12\text{-AS}_w](\text{binomial } n = 2) = 8.0 \times 10^{-13}$ M). Since the experimental solubility of 12-AS in the pH = 6 buffer is $(5 \pm 3) \times 10^{-9}$ M, we can conclude that the solubility equilibrium in the aqueous phase is not responsible for the limited value of the mean occupation number in CTAC micelles. Following this experimental evidence, the fact that both the fluorescence decay and the photodimerization of 12-AS are modeled by a Poisson distribution and do not fit a binomial distribution for a concentration up to 1.6×10^{-3} M ($\mu = 1.6$) remains unexplained.

As an alternative to a Poisson distribution, Hunter and co-workers proposed a different statistical distribution that better describes the solubilization of pyrene in CTAB micelles^{34,35} based on the assumption that the probe is not soluble in the water pseudophase but is always associated with surfactant molecules. As a consequence, the exit rate of the probe from the micelle is only dependent on the surfactant dynamics; that is, the exit rate is independent of the number of probe molecules present in that micelle. For a given mean occupation number the concentration of micelles with more probe molecules is higher than the one predicted from a Poisson distribution, increasing the overall perturbation of the micelle pseudophase. The fit of this model to our experimental results is not as good as that using a Poisson distribution, and the recovered rate constants are strongly concentration dependent. To overcome the enrichment of the micelle population with higher occupation numbers, the maximum number of molecules per micelle can be limited, but this is a further complication of the model that is not justified in our work since the simpler model based on the Poisson distribution describes the experimental results quite accurately.

The exit rate constant of 12-AS from CTAC micelles as been found to be ca. 10^{-3} s^{-1} . Since the surfactant is cationic and the stearic acid mostly ionized at pH = 6, an efficient aggregation of 12-AS to the micelle is to be expected. There are no exit rate constants for this type of compound in the literature that allow a direct comparison, but the exit rate constant from CTAB for nonionic aromatic compounds ranges from 10^2 to $5 \times 10^3 \text{ s}^{-1}$.^{36,37} Our value seems reasonable given the difference of charge.

The assumption that the entrance rate is diffusion controlled deserves discussion. For example the rate of entrance of neutral arenes in SDS micelles is half of what would be expected from diffusion control.³⁶ For the association of the anionic 12-AS with the cationic CTAC micelle the assumption made seems reasonable; the same may not be true with the nonionic C₁₂E₁₀ micelles. However, in our case, the decrease of k^+ leads to a concomitant increase of $[12\text{-AS}_w]$, and the overall entrance rate is not significantly affected. For $k^+ \geq 1 \times 10^8 \text{ M}^{-1} \text{ s}^{-1}$ the solubility limit will not be attained.

Conclusions

The commonly accepted positive catalytic effect produced by micelle solutions is in fact a consequence of the increased effective concentration. If a comparison is made for equivalent concentrations, compartmentalization leads to an inhibition of bimolecular reactions as for the case of photodimerization shown in this work. This inhibition results from two factors: first, for photochemical reactions with long-lived species ($\tau > R_M^2/3D$) the shortness of reactants within the mean displacement distance decreases the probability of reaction; second, the depletion of available reactants as reaction proceeds is more pronounced in compartmentalized media.

The first effect, mean displacement distance larger than compartment linear dimension, results in a time-independent apparent rate constant, k_{app} , as shown in Figure 5b (---), while the depletion of reactants, which develop a nonrandom molecular distribution, results in a time-dependent apparent rate constant.

Interchange of reactants between micelles leads to a randomization. In the limiting situation for which a significant interchange takes place during the excited molecule lifetime, neither of the compartmentalization effects will be apparent. However in the more general case in which the excited state lifetime is very short as compared with the interchange of reactants between compartments, the reaction will be hindered.

From this work it becomes clear that even for systems where an interchange between compartments results in a relatively fast reagent randomization, the observed photochemical kinetics are so different from those obtained in homogeneous media that a complete treatment, such as the one presented here, is absolutely necessary.

Acknowledgment. The research described herein was supported by JNICT contracts PBIC/CEN/1088/92 and PMCT/CEN/658/90. M.J.M. is indebted to JNICT-Portugal for Grant BD/1028/90-IF.

References and Notes

- (1) Kalyanasundaram, K. *Photochemistry in Organized & Constrained Media*; Ramamurthy, V., Ed.; VCH Publishers, Inc.: New York, 1991; Chapter 2.
- (2) Melo, E.; Costa, S. M. B. *J. Chem. Soc., Faraday Trans.* **1990**, 86, 2155–2162.
- (3) Tachiya, M. *Kinetics of Nonhomogeneous Processes*; Freeman, G. R., Ed.; J. Wiley & Sons: New York, 1987; Chapter 11, p 575.
- (4) Maestri, M.; Infelta, P. P.; Graetzel, M. *J. Chem. Phys.* **1978**, 69, 1522.
- (5) Bunton, C. A. *Kinetics and Catalysis in Microheterogeneous Systems*; Grätzel, M., Kalyanasundaram, K., Eds.; Marcel Dekker Inc.: New York, 1991; p 13.
- (6) Costa, S. M. B.; Melo, E. *J. Chem. Soc., Faraday Trans. 2* **1980**, 76, 1.
- (7) Cowan, D. O.; Drisko, R. L. *Elements of Organic Photochemistry*; Plenum Press: New York, 1976; p 37.
- (8) Cowan, D. O.; Schmiegell, W. W. *J. Am. Chem. Soc.* **1972**, 94, 6779.
- (9) Robertson, W. W.; Music, J. F.; Matsen, F. A. *J. Am. Chem. Soc.* **1950**, 72, 5260.
- (10) Yamamoto, S.-A.; Grellmann, K.-H.; Weller, A. *Chem. Phys. Lett.* **1980**, 70, 241.
- (11) Yang, N. C.; Shold, D. M.; Kim, B. *J. Am. Chem. Soc.* **1976**, 98, 6587.
- (12) Melo, E.; Costa, S. M. B.; Maçanita, A. L.; Santos, H. J. *Colloid Interface Sci.* **1991**, 141, 439.
- (13) Wolff, T.; Suck, T. A.; Emming, C.-S.; Von Bunau, G. *Progr. Colloid Polym. Sci.* **1987**, 73, 18.
- (14) Hatlee, M. D.; Kozak, J. J. *J. Chem. Phys.* **1981**, 74, 5627.
- (15) Melo, E. C. C.; Lourtie, I. M. G.; Sankaram, M. B.; Thompson, T. E.; Vaz, W. L. C. *Biophys. J.* **1992**, 63, 1506.
- (16) Almgren, M.; Lofroth, J.-E. *J. Colloid Interface Sci.* **1981**, 81, 486.
- (17) Gear, C. W. *Numerical Initial Value Problems in Ordinary Differential Equations*; Prentice-Hall, Inc.: Englewood Cliffs, NJ, 1971.

- (18) Malliaris, A.; Lang, J.; Zana, R. *J. Chem. Soc., Faraday Trans. 1* **1986**, 82, 109.
- (19) Offen, H. W.; Dawson, D. R.; Nicoli, D. F. *J. Colloid Interface Sci.* **1981**, 80, 118.
- (20) Sato, T.; Saito, Y.; Anazawa, I. *J. Chem. Soc., Faraday Trans.* **1988**, 84, 275.
- (21) Quantum Chemistry Program Exchange, Indiana Univ. package nr 11.
- (22) Maçanita, A. L.; Costa, F. P.; Costa, S. M. B.; Melo, E. C.; Santos, H. *J. Phys. Chem.* **1989**, 93, 336.
- (23) Atik, S. S.; Nam, M.; Singer, L. A. *Chem. Phys. Lett.* **1979**, 67, 75.
- (24) Wolff, T.; Muller, N.; Von Bunau, G. *J. Photochem.* **1983**, 22, 61.
- (25) Rothenberger, G.; Infelta, P. P. *Kinetics and Catalysis in Micro-heterogeneous Systems*; Grätzel, M., Kalyanasundaram, K., Eds.; Marcel Dekker Inc.: New York, 1991; p 52.
- (26) Malliaris, A.; Boens, N.; Luo, H.; Van Der Auweraer, M.; de Schryver, F. C.; Reekmans, S. *Chem. Phys. Lett.* **1989**, 155, 587.
- (27) Shon, R. S.-L.; Cowan, D. O.; Schmieg, W. W. *J. Phys. Chem.* **1975**, 79, 2087.
- (28) Costa, S. M. B.; Maçanita, A. L. *J. Photochem.* **1979**, 11, 429.
- (29) Henderson, C. N.; Selinger, B. K.; Watkins, A. R. *J. Photochem.* **1981**, 16, 215.
- (30) Maçanita, A. Private communication.
- (31) Melo, E. Ph.D. Thesis, Universidade Técnica de Lisboa, Lisboa, Portugal, 1986.
- (32) Stevens, B. *Adv. Photochem.* **1971**, 8, 161.
- (33) Warr, G. G.; Grieser, F. *Chem. Phys. Lett.* **1985**, 116, 505.
- (34) Dorrance, R. C.; Hunter, T. F. *J. Chem. Soc., Faraday Trans.* **1974**, 70, 1572.
- (35) Hunter, T. F. *Chem. Phys. Lett.* **1980**, 75, 152–155.
- (36) Almgren, M.; Grieser, F.; Thomas, J. K. *J. Am. Chem. Soc.* **1979**, 101, 279.
- (37) Infelta, P. P.; Gratzel, M.; Thomas, J. K. *J. Phys. Chem.* **1974**, 78, 190.

JP9614660